



HAL
open science

Hygrothermal properties of light-earth building materials

Thibaut Colinart, Théo Vinceslas, H el ene Lenormand, A. Hellouin de Menibus, Erwan Hamard, Thibaut Lecompte

► **To cite this version:**

Thibaut Colinart, Th eo Vinceslas, H el ene Lenormand, A. Hellouin de Menibus, Erwan Hamard, et al.. Hygrothermal properties of light-earth building materials. *Journal of Building Engineering*, 2020, 29, pp.101134. 10.1016/j.job.2019.101134 . hal-03008232

HAL Id: hal-03008232

<https://hal.science/hal-03008232>

Submitted on 3 Jun 2021

HAL is a multi-disciplinary open access archive for the deposit and dissemination of scientific research documents, whether they are published or not. The documents may come from teaching and research institutions in France or abroad, or from public or private research centers.

L'archive ouverte pluridisciplinaire **HAL**, est destin ee au d ep ot et  a la diffusion de documents scientifiques de niveau recherche, publi es ou non,  emanant des  tablissements d'enseignement et de recherche fran ais ou  trangers, des laboratoires publics ou priv es.

Hygrothermal properties of light-earth building materials

T. COLINART^{1*}, T. VINCESLAS¹, H. LENORMAND², A. HELLOUIN DE
MENIBUS^{3,4}, E. HAMARD⁵, T. LECOMPTE¹

¹ Univ. Bretagne Sud, UMR CNRS 6027, IRDL, F-56100 Lorient, France

² UniLaSalle, EA7519 (UniLaSalle Université d'Artois) F-76134 Mont-Saint-Aignan

³ Eco-Pertica, Hôtel Buissonnet, F-61340 Perche-en-Nocé

⁴ Association Nationale des Chanvriers en Circuits Courts, Hôtel Buissonnet, F-61340
Perche-en-Nocé

⁵ IFSTTAR, MAST, GPEM, F-44344 Bouguenais

Corresponding author:

Thibaut COLINART

IRDL – Université de Bretagne Sud

Rue de saint Maudé, BP 92116,

56321 Lorient Cedex, France

Phone: 33/0 2 97 87 45 17

Fax: 33/0 2 97 87 45 72

Mail : thibaut.colinart@univ-ubs.fr

Abstract

This experimental study provides complete datasets of hygrothermal properties of numerous hemp-clay with density ranging from 200 to 350 kg.m⁻³ for building thermal insulation. In addition, attention is also paid on protocols and methods, on the measurements repeatability and on the influence of conditioning temperature and relative humidity: mean uncertainties do not exceed 10 % for all measurements, while initial conditioning influences at most the results, particularly for the sorption isotherm. Heat and moisture storage properties depend obviously of the constituent (hemp or clay). Furthermore, they can be estimated with a good accuracy with a mixing law. Thermal conductivity of the composites ranges between 0.06 and 0.12 W.m⁻¹.K⁻¹ and clearly depends on the density. Water vapor diffusion resistance factor ranges between 2.24 and 4.14, while capillary absorption coefficient ranges between 0.027 and 0.135 kg.m⁻².s^{-0.5}.

Keywords

Sorption isotherm; specific heat capacity; thermal conductivity; water vapor diffusion resistance factor; capillary absorption coefficient; hemp shiv; clay; light-earth;

Highlights

- Mean experimental errors do not exceed 10 %.
- Drying temperature and relative humidity are the most influencing parameters.
- Mixing law are validated for estimating heat and moisture storage properties.
- Thermal conductivity ranges between 0.06 and 0.12 W.m⁻¹.K⁻¹.
- Water vapor diffusion resistance factor ranges between 2.24 and 4.14.
- Capillary absorption coefficient ranges between 0.027 and 0.135 kg.m⁻².s^{-0.5}.

Introduction

In a context of sustainable building, bio-based building materials, among them bio-based concretes or mortars, has gained interest in the last two decades. These materials are made of plant aggregates (hemp, flax, sunflower, etc. [1-2]) and binder (mineral binder like lime or cement, natural binder like earth). Compared to cement concrete, they are more porous, lighter (density ranging from 200 to 1200 kg.m⁻³) and present lower thermal conductivity (ranging from 0.05 to 0.2 W.m⁻¹.K⁻¹). One other major feature of these materials is that they are hygroscopic, i.e. they can catch/release moisture from/to its surrounding. This moisture buffering potential could help in smoothing indoor relative humidity variations and improving comfort [3]. However, moisture affects other functional properties, like thermal [4] or acoustic properties [5], and may be a source of pathology [6]. Therefore, predicting the hygrothermal behavior of these materials in use is relevant. Simulations are generally performed with software like WUFI [7] or Delphin [8] or other Heat, Air and Moisture transfer models [9]. Whatever the model, numerous input data are required, at least dry thermal capacity and conductivity, sorption isotherm, vapor and liquid transfer properties.

From now, hygrothermal characterization of lime and hemp concrete received the most attention [10-18]. Broadly speaking, the studies investigate the influence of formulation, setting process, constitutive materials (plant aggregate and binder type) or external parameters like temperature and relative humidity. Because lime has a great impact on the life-cycle analysis of hemp-lime concrete [19], alternative binders are investigated. Among them, clay (and by extension earth) is increasingly studied because of its local availability and low environmental impact. As highlighted by Laborel-Préneron et al. [20], the use of plant aggregates in earthen constructions is not new: in most of the tested materials, plant aggregate

content is rather low leading to a density higher than 800 kg.m^{-3} . On the other hand, few studies deal with low density earthen construction materials [3,21-26]. A summary of measured hygrothermal properties is gathered in Table 1. In all studies, thermal conductivity is measured: excepted the value measured by Goodhew and Griffiths [21], all values range between 0.055 and $0.13 \text{ W.m}^{-1}.\text{K}^{-1}$ and increase linearly with density [3,25,26]. Nevertheless, the direct comparison between these values is difficult for at least three reasons: plant aggregates are not the same, measurements are performed at different conditions (dry state or ambient conditions, different measurement temperature) and different measurement methods may be used. Other properties are punctually evaluated. No direct measurement of specific capacity is done and recalculated values from thermal diffusivity are spread. Sorption isotherms present a sigmoidal shape and moisture content at 80 %RH range between 4.8 and 8 %. Vapor diffusion resistance factor is rather small and has the same order of magnitude than the one of lime and hemp concrete. Last, let note that no capillary absorption measurement has been done. This review indicates that complete datasets are rather scarce in the literature. In addition, it does not allow to determine the most influencing parameters on the hygrothermal properties. Indeed, plant aggregates have intrinsic properties which may influence the hygrothermal behavior of the composite [2]. Similarly, raw earth presents variabilities in terms of particle size distribution, clayey behavior and chemical components for instance [27]. In the case of earth bricks, Cagnon et al. [28] have shown that this variability influences the heat and moisture storage properties.

In this paper, we aim to provide a complete dataset of hygrothermal properties of light-earth building materials. In addition, the influence of earth variability is discussed and compared to other sources of variability. Particularly, a focus is done on the drying conditions and in its influence on the hygrothermal properties. In this view, the paper is divided as

follows: Section 2 and Section 3 present respectively materials and methods. Heat and moisture storage properties are presented and discussed in Section 4, while thermal and hydric transfer properties are analyzed in Section 5.

Ref	Plant aggregate	ρ [kg.m ⁻³]	λ [W.m ⁻¹ .K ⁻¹]	c_p [J.kg ⁻¹ .K ⁻¹]	μ [-]	w_{80} [%]	MBV [g.m ⁻² .%RH ⁻¹]
[21]	Straw	440	0.18	900			
[22]	Hemp-shiv	420	0.13	1666*			
[3]	Straw	241 ... 531	0.071 ... 0.12		4.8 (dry) 2.9 (wet)	4.8 ... 5.5** (drying: 55 °C)	
[23]	Hemp-shiv	385	0.085				2.68
[24]	Straw	356	0.072				
[25]	Typha (3 form.)	304 ... 586	0.065 ... 0.112	910 ... 960*	3.2 ... 7.1 (dry) 1.3 ... 2.5 (wet)	≅ 6 ... 8 %** (drying: 50 °C)	3.23 ... 4.3
[26]	Rape-Straw Sunflower-shiv	235 ... 512	0.055 ... 0.088 (+ increase with RH)			≅ 6 %** (drying: 60 °C)	

*Table 1: Overview of previous measured hygrothermal properties on light earth materials for building
(* calculated value from thermal diffusivity; ** value estimated from figure reading).*

1 Materials

1.1 Earth

Six soils were collected in West France (see Figure 1). One reference (REF or E0) had already been used by builders on more than 15 hemp-earth constructions. The others (E1 to E5) were chosen among 26 soils in order to cover the diversity of earth encountered in West France.

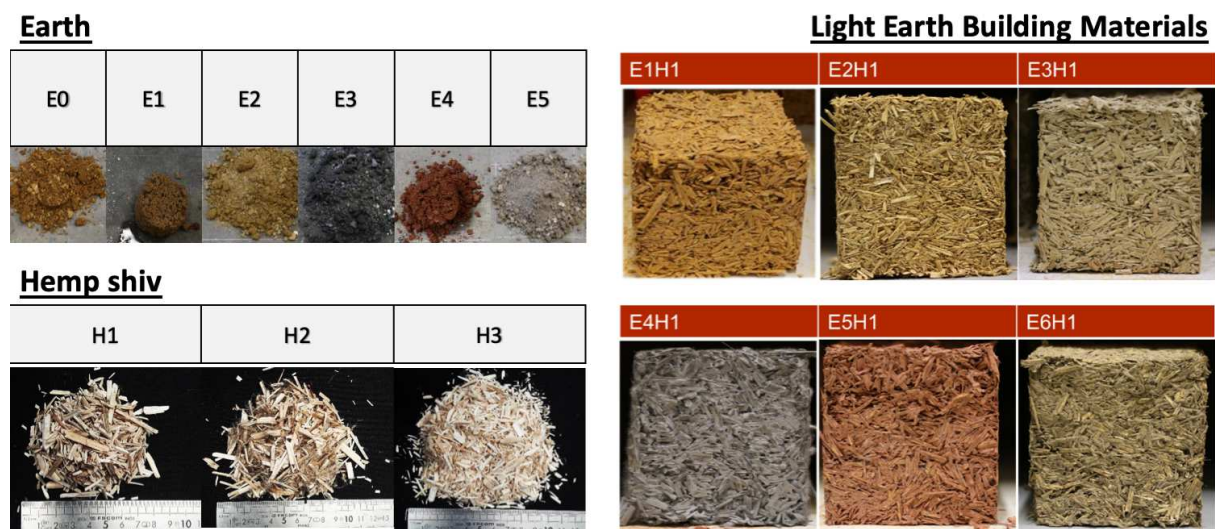


Figure 1: Overview of earth, hemp shiv and light earth building materials.

Classical geotechnical characterizations were performed by Vincelas et al. [29]. Particles size distribution was evaluated by sedimentation and sieving according to the standard ISO 17892-4 to quantify the mass fractions of clay, silt and sand. Specific density is evaluated according the standard ISO 17892-3. Cation Exchange Capacity *CEC* was measured with cobalt hexamine according to ISO 23470 to quantify exchangeable cations sites on clay, which are linked to specific surface and binding capacity [30]. Clay mineralogy has been determined by X-Ray Diffraction according to the protocol of Chen [31].

Results are summed up in Table 2. They show the large range of variabilities observed for the particle size distribution or the Cation Exchange Capacity CEC. E0 and E3 are noteworthy, since earth with 50 % of clay or more is uncommon [27]. E1 is very granular and presents a low fines content. E5 presents the largest CEC, with a relative low amount of clay. Specific densities range from 2575 to 2821 kg.m⁻³. All tested earth present Chlorite, Illite and Kaolinite. E4 contains also Vermiculite while E3 and E5 contains Pyrophyllite.

		Standard	REF/E0	E1	E2	E3	E4	E5
Clay (0 – 2 µm)	[%]	ISO 17892-4	51	10	25	47	40	18
Silt (2 – 50 µm)	[%]		32	7	32	51	30	63
Sand (50 µm – 2 mm)	[%]		17	83	43	2	30	19
ρ_{earth}	[kg.m ⁻³]	ISO 17892-3	2661	2714	2821	2810	2806	2575
CEC	[cmol ⁺ .kg ⁻¹]	ISO 23470	14	4	5	7	13	21
Clay type*			Chl., Illi., Kao.	Chl., Illi., Kao.	Chl., Illi., Kao.	Chl., Illi., Kao., Pyr.	Chl., Illi., Kao., Ver.	Chl., Illi., Kao., Pyr.

Table 2: Geotechnical characteristics of the six soils.

(* Chl.: Chlorite, Illi.: Illite, Kao.: Kaolinite, Ver.: Vermiculite, Pyr.: Pyrophyllite)

1.2 Hemp shiv

Three hemp shiv are tested in this work (see Figure 1). H1 and H2 are coming from the same batch. They are produced in the Normandy Region in France. The variety is FEDORA

17, sowed at 50 kg/ha, harvested in autumn and defibered in a local producer transformation unit [32]. H3 is a commercial product produced elsewhere in France.

For each hemp shiv, particles size distribution and bulk density are evaluated according to [33], specific density is measured by pycnometry and chemical composition is determined by the Van Soest method.

The difference observed in the chemical composition are not significant. H1 and H2 present different morphologies: average particle dimension and bulk density are higher for H2 than for H1. H3 shiv are slightly smaller, leading to higher bulk density.

		H1	H2	H3
Av. width	[mm]	1.6	2	1.5
Av. length	[mm]	6.3	8.6	6.1
Elongation	[-]	4.3	4.7	4.2
Bulk density	[kg.m ⁻³]	99.6	103.5	122.4
Specific density	[kg.m ⁻³]	1497	1492	1484
Cellulose	[%]	60.4	62.5	59.9
Hemicellulose	[%]	13.8	16.5	20.7
Lignin/cutin	[%]	16.2	15.4	13.9
Extractives	[%]	9.7	5.7	5.5

Table 3: Hemp shiv characteristics.

1.3 Light earth building materials

Light earth building materials is obtained by mixing hemp shiv and earth slip. Here, earth slips are prepared as follows [34]: raw soils are mixed with water until liquid state is reached

to permit their wet sieve with a 2 mm square sieve to remove coarse particles; then, water is added to reach viscosity level considered as acceptable for light earth construction [34].

In this work, two batches are prepared with a craftsman, to ensure its representativeness with regard to the material used in building works. The first batch is prepared with reference earth E0 and aims to evaluate the influence of hemp shiv. In addition, samples E0H1(L) are prepared with a higher hemp mass fraction to evaluate the influence of the formulation and samples E0H1(S) are made by spraying to evaluate the influence of the setting process. The second batch is prepared with hemp shiv H1 and aims to evaluate the influence of earth. In this case, earth slips are prepared according to two methods: equivalent water/earth ratio (samples a) or equivalent rheology of all earth slips (samples b). Hemp mass fraction f_{hemp} of the 15 mixtures are gathered in Table 4. A view of six samples is proposed in Figure 1.

Samples are prepared by filling up cubic molds with dimensions of $100 \times 100 \times 100 \text{ mm}^3$ in five layers with equal mass of fresh material. They are unmolded straight after their fabrication and dried at room conditions ($23 \pm 2 \text{ }^\circ\text{C}$, $50 \pm 10 \text{ \%RH}$). A final drying is performed at $70 \text{ }^\circ\text{C}$ in a ventilated oven to assess the dry density ρ_{dry} (see Table 4). Last, compactness C is defined as:

$$C = \frac{V_{earth} + V_{hemp}}{V_{sample}} = \rho_{dry} \left(\frac{1 - f_{hemp}}{\rho_{earth}} + \frac{f_{hemp}}{\rho_{hemp}} \right) \quad (1)$$

with ρ_{hemp} the intrinsic density of hemp shiv. Porosity is defined as the opposite to the compactness.

Hemp mass fraction f_{hemp} is around $42 \pm 2 \text{ \%}$, except for four samples: samples E0H1(L) are prepared deliberately with a high amount of hemp; sprayed samples E0H1(S) present a lower amount of hemp since the craftsman wanted to insure a better cohesion at fresh state by adding earth slip; Particularly, we note that sample of similar density can obtained either by adding hemp shiv and compacting the sample or by spraying and adding more earth slip; Last, samples E1H1a and E5H1b differ from the mean value because of difficulties in the earth slip

preparation. In general, dry density and compactness of all samples range between 196 and 345 kg.m⁻³ and 10.7 and 17 % respectively. In addition, both are linearly dependent in the investigated range. Samples made with earth with low amount of clay and silt are crumblier than others: each handling induces mass loss, which increases the uncertainty.

	Name	Hemp mass fraction f_{hemp} [%]	Dry density ρ_{dry} [kg.m ⁻³]	Compactness C [%]	Porosity [%]
Batch 1	E0H1	42.2 ± 0.4	304 ± 6	14.9 ± 0.3	85.1 ± 0.3
	E0H2	44 ± 0.4	283 ± 2	14.1 ± 0.1	85.9 ± 0.1
	E0H3	42.2 ± 0.4	345 ± 13	17 ± 0.7	83 ± 0.7
	E0H1(L)	52.9 ± 0.4	205 ± 8	10.7 ± 0.4	89.3 ± 0.4
	E0H1(S)	33.7 ± 0.3	272 ± 26	12.7 ± 1.2	87.3 ± 1.2
Batch 2	E1H1a	67 ± 0.4	196 ± 34	11.1 ± 1.9	88.9 ± 1.9
	E1H1b	41.4 ± 0.4	238 ± 24	11.7 ± 1.2	88.3 ± 1.2
	E2H1a	42.3 ± 0.4	236 ± 4	11.5 ± 0.2	88.5 ± 0.2
	E2H1b	42.2 ± 0.4	281 ± 1	13.7 ± 0.1	86.3 ± 0.1
	E3H1a	43.4 ± 0.4	272 ± 8	13.4 ± 0.4	86.6 ± 0.4
	E3H1b	43 ± 0.4	263 ± 15	12.9 ± 0.7	87.1 ± 0.7
	E4H1a	43.4 ± 0.4	252 ± 3	12.4 ± 0.2	87.6 ± 0.2
	E4H1b	41.5 ± 0.4	257 ± 2	12.4 ± 0.1	87.6 ± 0.1
	E5H1a	42.7 ± 0.4	258 ± 18	13.2 ± 0.9	86.8 ± 0.9
	E5H1b	37.5 ± 0.4	307 ± 7	15.3 ± 0.4	84.7 ± 0.4

Table 4: Tested formulations.

2 Methods

2.1 *Preliminary remarks on dry state*

When characterizing hygrothermal properties of hygroscopic building materials, dry state should generally be defined either to measure properties at this state (thermal capacity, thermal conductivity) or to assess dry mass to evaluate moisture content. Usually, drying is performed in ventilated oven in accordance with the standard ISO 12570 [35-37]. The latter mentions that drying temperature should be set to the one specified in the product standard or by default to 40, 70 (recently reduced to 65) or 105 ± 2 °C depending on materials sensitivity to temperature. However, product standards recommend drying temperature ranging from 40 °C [38] to 110 °C [39] for earth-based materials and from 70 °C [40] to 103 °C [41] for cellulosic-based materials. In addition, the standard ISO 12570 mentions that the relative humidity should be maintained below 10 %RH. Since the air in the oven is frequently the same air as in the lab, relative humidity in the oven depends therefore on the laboratory climate [42]: for instance, assuming that air vapor contents are 7 and 14 g.m⁻³ respectively in wintertime and in summertime, relative humidity varies from 1 to 2 %RH when drying temperature is 105 °C, but from 16 to 30 %RH when drying temperature is 40 °C.

Consequently, numerous drying conditions (in terms of temperature and relative humidity) can be encountered in the literature dealing with bio-based building materials. This leads to spread values of hygrothermal properties for which a direct comparison is therefore difficult. In this work, attention is paid in the drying conditions and in its influence on the hygrothermal properties.

2.2 Storage properties

2.2.1 Sorption isotherm

Saturated Salt Solution (SSS) method

Sorption isotherms are measured by gravimetric method according to the standard ISO 12571 [43]. For each material, samples representative of the product with a mass of at least 10 g are placed on glass cups. As hemp shiv particles have dry apparent density of less than $300 \text{ kg}\cdot\text{m}^{-3}$, the weighing cups have an area of at least $100 \times 100 \text{ mm}^2$. For light earth building materials, cubic samples with dimensions of at least $50 \times 50 \times 50 \text{ mm}^3$ are prepared. Then, samples are dried prior to sorption experiments. Based on the above-mentioned discussion (see Section 3.1), three different drying protocols are tested:

- Initial drying at $105 \text{ }^\circ\text{C}$ in a ventilated oven (in winter or in summer),
- Initial drying at $40 \text{ }^\circ\text{C}$ in a ventilated oven (in winter or in summer),
- Initial drying at $40 \text{ }^\circ\text{C}$ and 20 \%RH in a climatic chamber.

Constant mass is assumed to be reached when the weight change between two consecutive weightings made 24 hours apart is less than 0.1 \% of the total mass. Then, sample are placed until mass equilibrium in desiccators equipped with fans in which relative humidity is controlled by saturated salt solutions. Four to eight relative humidity increasing in stages are tested, the temperature being maintained at $23 \pm 0.5 \text{ }^\circ\text{C}$.

Dynamic Vapor Sorption (DVS) method

Sorption isotherms of reference earth E0 and hemp shiv H1 are also measured with the DVS equipment IGASorp-HT system (Hiden Analytical, Warrington, UK). The device allows monitoring the mass uptake and the sorption kinetics of one sample accurately by means of a microbalance and precise control of both temperature and humidity. The protocol is the following. 10 to 100 mg of material is placed in the IGAsorp microbalance, which has

resolution of 0.1 μg . Prior to the start of the adsorption analysis, the sample is first dried in flowing air (250 mL/min) to a constant weight. Here, two drying protocols are tested: 40 °C / 20 %RH and 105 °C / RH < 1 %. Then, the sample is exposed to increasing humidity from 10% to 90%, in 10% humidity steps, the testing temperature being 23 °C. The equilibrium mass at each step is determined by extrapolation of a single exponential curve fit to the time-dependent mass response following a step change in RH.

2.2.2 Specific heat capacity

The specific heat capacity measurements are carried out using a micro-DSC III calorimeter (Setaram, Calluire, France) according to the standard ISO 11357-4 [44]. A minimum mass of 100 mg is placed in 1 cm³ sealed vessels. For light earth building materials, random sampling of few particles is done. A continuous method is mainly applied for which temperature is increased from 5 °C to 30 °C using a heating rate of 0.2 °C.min⁻¹. Results are punctually compared to the ones obtained by a stepwise method for which temperature is increased from 15 °C to 25 °C using a heating rate of 0.2 °C.min⁻¹. Measurements are made on all materials dried according the above-mentioned drying protocols.

When possible, three measurements were performed on each material for both storage properties measurement. If not, the results are discussed regarding the uncertainties.

2.3 Transfer properties

2.3.1 Thermal conductivity

Thermal conductivity λ is measured using home-made guarded hot plate device [45] according to the EN 12664 standard [46]. Tests are made on samples with mean dimensions of 100 x 100 x 50 mm³. Prior testing, specimens are dried at 70 °C in ventilated oven and cold in desiccant at room temperature. They are then clamped between cold and hot plates to

improve contacts and to minimize interface-resistance errors. Measurements are performed at a mean temperature of 23 °C by setting cold and hot temperature respectively to 18 ± 0.05 and 28 ± 0.05 °C. In addition, insulating material is placed around the samples to limit heat losses during the test. Once steady state is reached for the dissipated heat flux, an apparent thermal conductivity λ is calculated by assuming one-dimensional conductive heat transfer. The influence of thermal interface resistance is discussed in Section 5. In addition, further measurements are done on some specimens either after drying at 40 °C in ventilated oven or after conditioning at 23 °C and 50 %RH in climatic chamber. Here, all measurements are performed in the direction of interest for use in building, i.e. perpendicularly to the direction of compaction or in the spraying direction for the sprayed sample.

2.3.2 Water vapor diffusion resistance factor

Water vapor diffusion resistance factor μ is measured using dry cup according to the ISO 12572 standard [47]. Tests are made on the same samples as for thermal conductivity. Prior testing, specimens are conditioned at 23 °C and 50 %RH. They are then sealed with aluminum tape to a PE cup containing silica gel as desiccant. Air layers between specimen and silica gel are 17 ± 3 mm thick. Relative humidity inside the cup is assumed equal to 5 %RH. Assemblies are placed in a climatic chamber at a temperature of 23 °C and 50%RH. Air velocity measured above the cup with a hot-wire anemometer is around $0.2 \text{ m}\cdot\text{s}^{-1}$. The cups are regularly weighed until water vapor transmission rate (g_v) reaches steady state. Water vapor diffusion resistance factor μ is calculated by accounting the additional resistance of air layers in and above the cup as specified in the Annex G of the standard.

2.3.3 Capillary absorption coefficient

Capillary absorption coefficient A_w is measured according to the ISO 15148 standard [48]. The experimental set-up is similar to the one of Fabbri et al. used for rammed earth [49]. Samples with dimensions of $100 \times 100 \times 100 \text{ mm}^3$ are initially stored in the lab and their lateral sides are sealed with cellophane to ensure one-dimensional moisture transfer. They are placed on a wire basket and then partially immersed into water to a depth of a 2-5 mm. After 5 min each test specimen was removed from the water, its surfaces blotted with a cloth and then weighed on balance reading 0.01 g. This procedure takes about 20 s and was repeated after 10, 15, 20, 25, 35, 45 min and 1, 2, 4, 24 h. All measurements are performed at room temperature, i.e. $23 \pm 2 \text{ }^\circ\text{C}$. Capillary absorption coefficient A_w is calculated from the slope between the amount of absorbed water per unit of sample surface and the square root of time.

3 Results and discussion on storage properties

3.1 Repeatability and influence of measurement method

Repeatability errors, defined as the ratio between standard deviation and mean value, and influence of measurement method are analyzed for all measurements. Mean and maximum errors are gathered in Table 5. Heat capacity of raw materials can be measured with a very good accuracy. Slightly higher dispersion is noted for light earth building materials: errors are rather due to sampling repeatability since each measurement requires only 1 cm³ of material. On the other hand, larger variabilities are observed for moisture contents measured with the SSS method even if the tested samples are representative of each material. This is due to two reasons: at first, mass variations are small regarding the weight-scale precision when relative humidity is low; secondly, it is rather difficult to maintain homogeneous relative humidity within desiccators, particularly for high relative humidity. Because of the high precision of the microbalance and because of the accurate control of ambient conditions, values obtained with the DVS method are therefore more repeatable. Last, significant deviations are observed between both measurement methods of sorption isotherms. It agrees with previous observations [28,50]. Since drying with DVS device is performed with dry gas, DVS method tends to provide higher moisture contents than SSS methods (see Annex 1). In the rest of the paper, only measurement obtained with SSS methods are provided because of data availability.

	Repeatability				Protocol	
	Cp (continuous)	Sorption SSS (RH < 75 %)	Sorption SSS (RH > 75 %)	Sorption DVS	Cp: continuous vs. stepwise	Sorption: SSS vs. DVS
Earth slip	0.5 % (< 1.05 %)	5 % (< 40.4 %)	3.7 % (< 12 %)	1.3 % (< 2.4 %)	0.2 % (< 0.3 %)	35.9 % (< 69.4 %)
Hemp Shiv	0.9 % (< 1.76 %)	8.4 % (< 14.2 %)	8.5 % (< 13.9 %)	2.7 % (< 9.5 %)	0.8 % (< 1 %)	26.3 % (< 63.7 %)
Light earth building materials	1.6 % (< 6.6 %)	9.6 % (< 34.8 %)	4.9 % (< 13 %)	-	-	

Table 5: Mean and maximum (in brackets) errors due to repeatability and measurement method for measurement of moisture content and dry specific heat capacity.

3.2 Influence of initial conditioning on constitutive materials

Dry specific heat capacity c_p and moisture content at $80 \pm 2 \%RH$ w_{80} of earth slips and hemp shiv are presented respectively in Figure 2 and Figure 3. Sorption isotherms of reference earth E0 and hemp shiv H1 are presented in Annex 1. Full datasets of all constitutive materials are available as supplementary materials.

Let first focus on the results obtained after conditioning at $40\text{ }^\circ\text{C}$ and $20\text{ } \%RH$ in a climatic chamber. For earth slips (Figure 2), c_p and w_{80} range respectively between 0.77 and $0.93\text{ J}\cdot\text{g}^{-1}\cdot\text{K}^{-1}$ and between 0.3 and 3.5 %. In the present range, specific heat capacity tends to increase with clay and silt fractions. Nevertheless, the variability of c_p is rather limited and similar to the one observed in the literature [51-52]. On the other hand, moisture content presents a wider range of variation. Particularly, it tends to increase with CEC: this is due to

large specific surface area on which moisture molecules can be adsorbed and to the availability of cation or charged sites around which moisture molecules can cluster [53]. Furthermore, Arthur [54] noted that clay mineralogy plays a role in moisture adsorption only above 75 %RH. Nevertheless, the measured values are similar to the ones observed in the literature.

For hemp shiv (Figure 3), lower differences are observed in c_p and w_{80} between materials since they present similar chemical compositions. The values of c_p ($1.35 \text{ J.g}^{-1}.\text{K}^{-1}$) are in the range of the ones of cellulose or lignin ($1.2 \text{ J.g}^{-1}.\text{K}^{-1}$) [55]. The mechanisms of moisture sorption are more complex: even if sorption capacity of lignin is lower than the one of cellulose and hemicellulose [56], sorption also depends also on the accessibility of sorption site and on the polymer mechanics at local scale (softening, swelling, relaxation) [57-58]. For the three hemp-shiv, w_{80} equals approximately 9 %. As H1 and H2 come from the same batch, differences can be attributed to natural variability of the plant. H3 show a slightly higher moisture content. Nevertheless, mold appeared for high relative humidity during the experiment: the composition and, thus, the hygroscopic behavior could be modified.

Then, we focus on the influence of initial conditioning on the results, i.e. the influence of drying temperature and the influence of relative humidity control during drying. As expected, the higher the drying temperature, the lower the dry mass, and thus the higher moisture content: w_{80} is one third higher for all hemp shiv, while the sensitivity of earth slips ranges between

38 % (E4) and 120 % (E1). Furthermore, by increasing drying temperature, more evaporable and even and non-evaporable water is expected to be removed. As specific heat capacity of water equals $4.18 \text{ J.g}^{-1}.\text{K}^{-1}$ and is higher than the one of other constituents, specific heat capacity of the material is therefore lower: an homogeneous decrease of 10 % is observed for all hemp shiv, while it ranges from 1 % (E1) to 8.5 % (E5) for earth slips. In addition, we

observe that not controlling relative humidity during drying stage lead to uncertainties up to 5.5 % (H1) for c_p and up to 43 % (E0) for w_{80} . While lowest values are measured during winter since ambient air is dried, values measured during summer depend on the moment of specimen sampling, i.e. in the morning or in the afternoon, explaining the different trend of H3. When compared to the repeatability uncertainties, the errors due to different conditioning are larger, which may explain the spread values encountered in the literature.

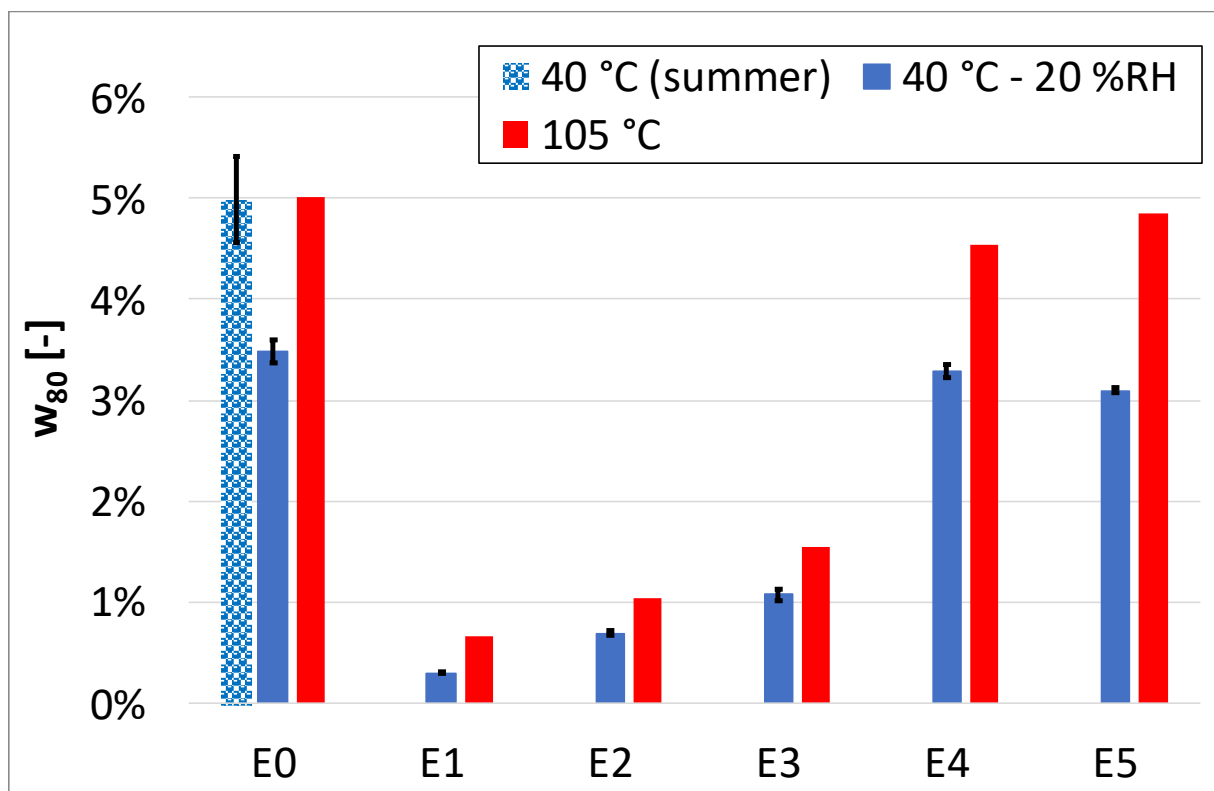
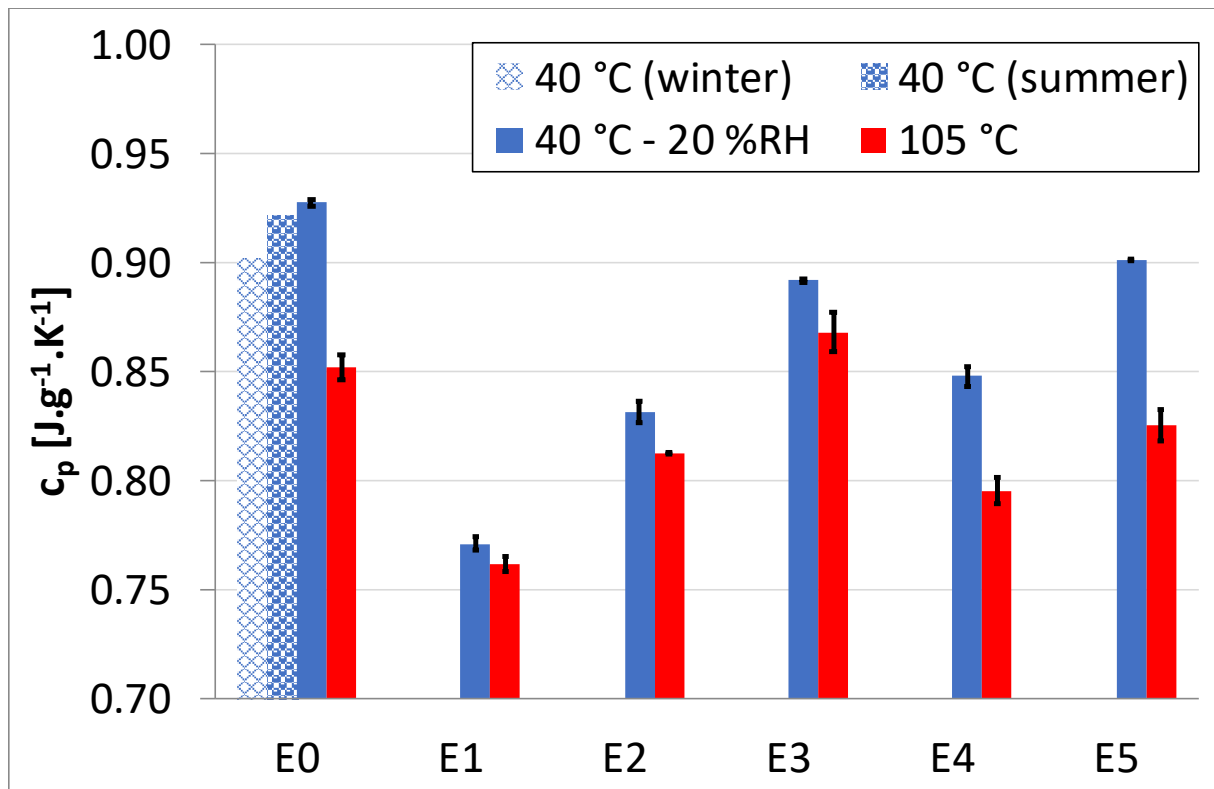


Figure 2: Dry specific heat capacity (a) and moisture content at 80 ± 2 %RH (b) of earth slips: influence of initial conditioning.

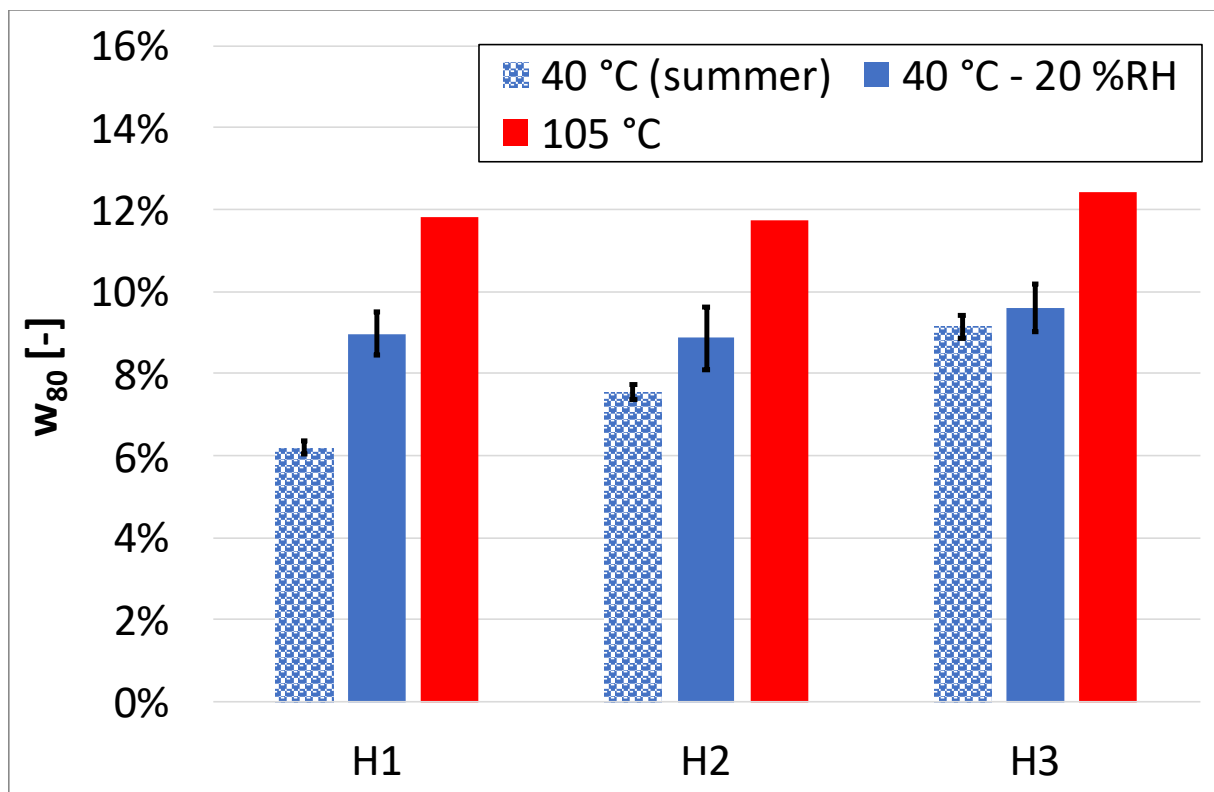
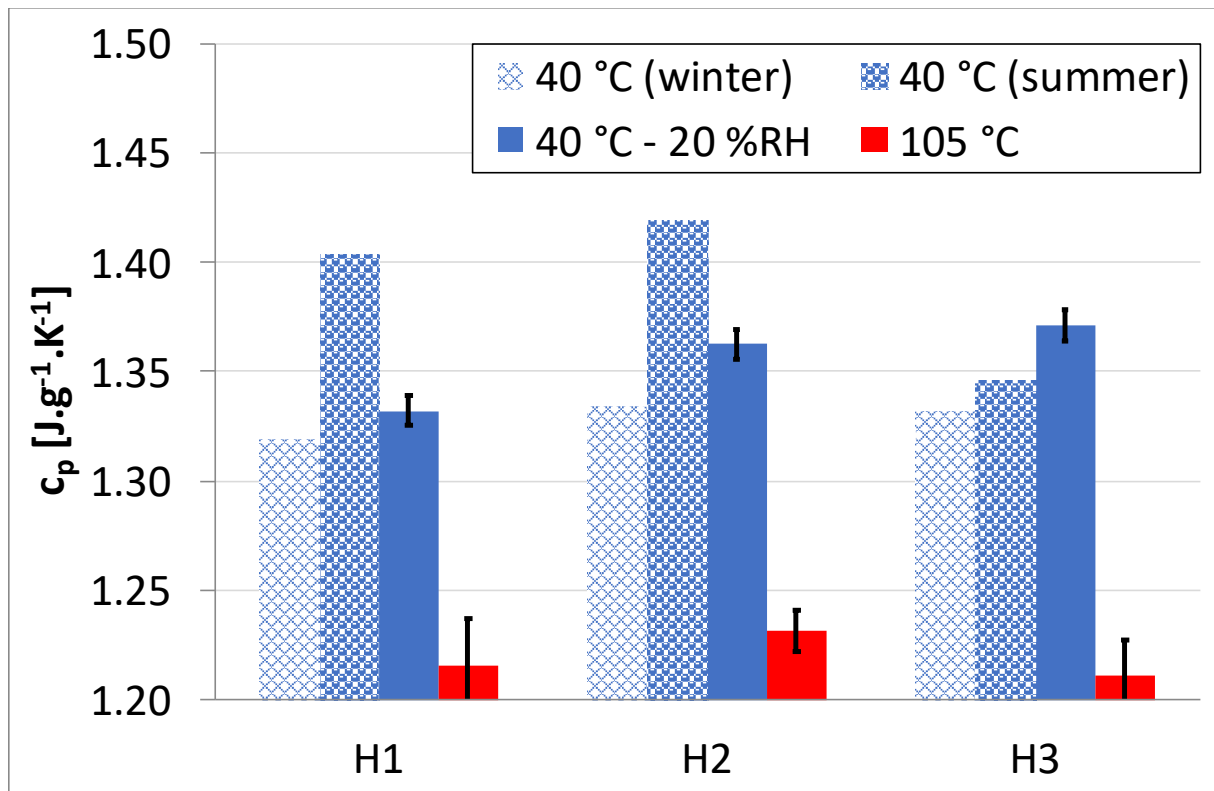


Figure 3: Dry specific heat capacity (a) and moisture content at $80 \pm 2\%$ RH (b) of hemp shiv: influence of initial conditioning.

3.3 Variability and validity of mixing law for light earth building materials

Dry specific heat capacity c_p and moisture content at 80 ± 2 %RH w_{80} of both batches of light earth building materials are presented in Figure 4. Sorption isotherms of sample EOH1 are presented in Annex 1. Full datasets of all materials are available as supplementary materials. All measurements are performed after conditioning either at 40 °C and 20 %RH in a climatic chamber or at 105 °C in ventilated oven, except sorption isotherms of batch 1.

For conditioning at 40 °C and 20 %RH in a climatic chamber, c_p ranges between 1.02 and 1.2 J.g⁻¹.K⁻¹. The material variability is about 3.5 %, which is slightly higher than repeatability error (1.61 %, see Table 5), but much lower than the influence of drying temperature (8.5 %). Regarding sorption, w_{80} of batch 2 ranges between 4.5 and 7 %, leading to a material variability of 16 %. Again, it is slightly higher than repeatability error (9.6 %, see Table 5) and in the same range than the influence of drying temperature (12.6 %).

These experimental data are compared to results obtained from a mixing law defined as:

$$c_{P,mix} = f_{hemp}c_{P,hemp} + (1 - f_{hemp})c_{P,earth} \quad (2)$$

$$w_{mix} = f_{hemp}w_{hemp} + (1 - f_{hemp})w_{earth} \quad (3)$$

with $c_{P,hemp}$ and w_{hemp} (resp. $c_{P,earth}$ and w_{earth}) dry specific heat capacity and moisture content of hemp shiv (resp. earth slips) measured previously. f_{hemp} is the mass fraction of hemp in the material (see Table 4). Since constitutive materials are in raw state when sample is prepared, the initial mass fraction should be recalculated at the appropriate drying temperature knowing the moisture content under ambient conditions. Therefore, error bars include uncertainties related to the mass fraction itself, but also the ones related to the measurement of moisture content of hemp shiv and of earth slip. An average difference of 1.96 % is observed for dry specific heat capacity: it is similar to repeatability error, validating thus the mixing law. Regarding moisture content, an average difference of 10 % is observed

for batch 2, minimum and maximum being 1 and 26 % respectively. On the other hand, larger differences are observed for batch 1: relative humidity was not controlled during drying and larger fluctuations of ambient conditions were noted during the experiment. Consequently, a rather good agreement can be observed between predicted and measured data considering all uncertainties, validating also the mixing law for moisture content in the hygroscopic range.

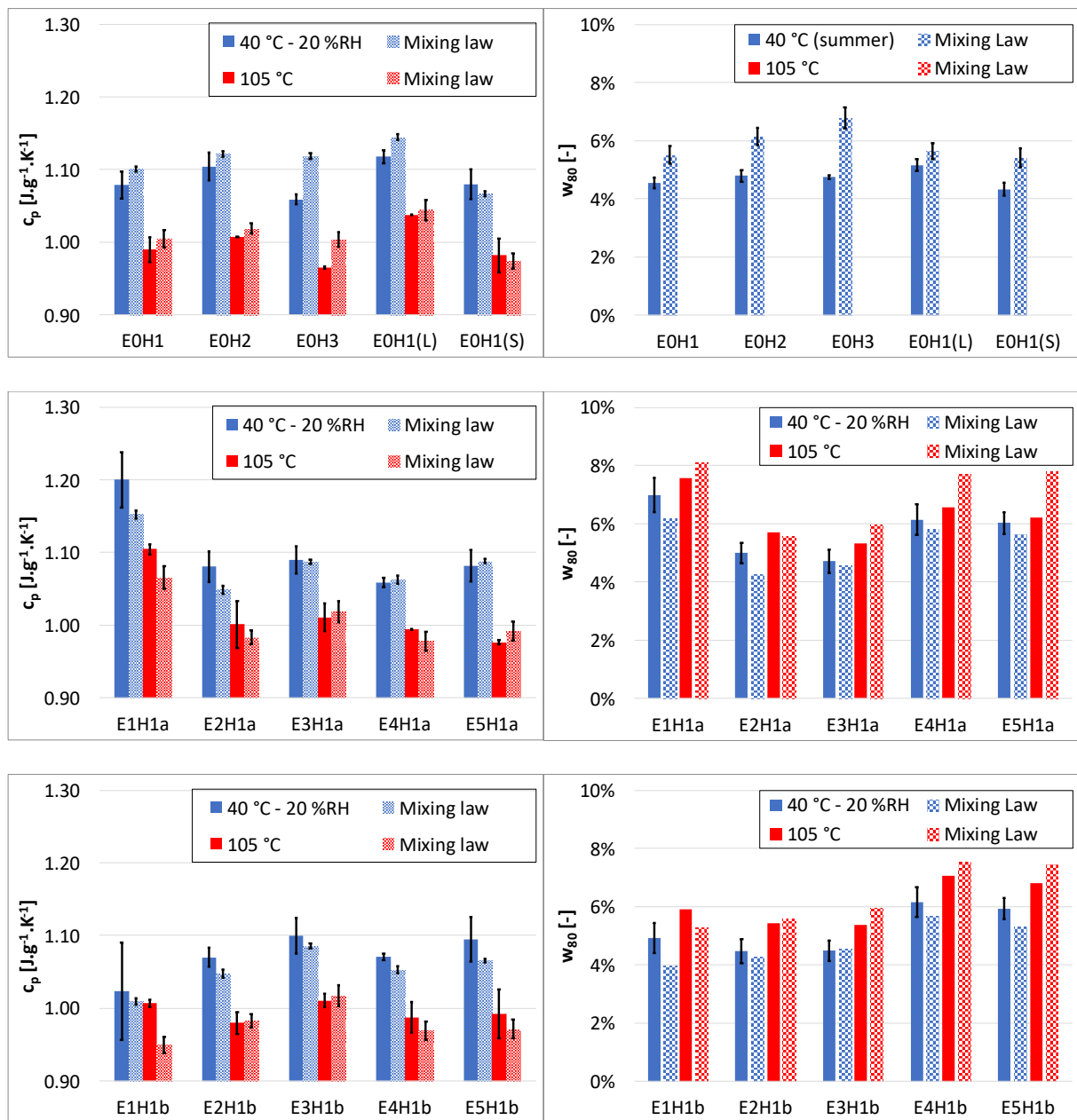


Figure 4: Dry specific heat capacity and moisture content at 80 ± 2 %RH for all samples of light earth building materials.

4 Results and discussion on transfer properties

4.1 *Uncertainties and repeatability*

Guarded hot plate and dry cup measurements are based on similar principles: a potential difference (temperature or relative humidity) is applied across a sample with given thickness and open surface which induces a flux (heat or moisture) through the sample and also through the interfaces. Transfer properties is deduced once steady state is reached. For both methods, mean and maximum uncertainty errors due to the dimensions, the potential accuracy and the interface resistance are gathered in Table 6 and compared to measurement's repeatability. Sample dimensions are measured with a vernier caliper by two operators. Since samples are heterogenous with rough surfaces, mean deviation of 1 % and 1.8 % are observed for the thickness and the surface. Mean uncertainties for both properties are therefore in the same range. The second uncertainty concerns the potential accuracy. For thermal conductivity measurement, temperatures are controlled with water baths. Furthermore, cold and hot plates have high thermal inertia. The uncertainty is rather due to temperature measurement which have a small effect on measured thermal conductivity. In the case of water vapor permeability measurement, ambient conditions are well controlled by the climatic chamber, contrary to the conditions within the cup: for instance, Pazera and Salonvaara [59] noted that relative humidity could increase by 5 %RH within 24 hours during the measurement of highly permeable construction materials. Here, assuming a relative humidity of 10 %RH (instead of 5 %RH) inside the cup may lead to non-negligible uncertainties up to 15 %. Last, the influence of interface resistance is discussed. For dry cup measurement, this point has been largely investigated in the literature [59-61]. Here, increasing interface resistance by $3.5 \cdot 10^7$ Pa.s.kg⁻¹ (which corresponds to the resistance of a 7 mm still air layer) induces a mean uncertainty of 4.35 % on the water vapor diffusion resistance factor. In the analysis of

guarded hot plate, contact thermal resistances are usually neglected. Nevertheless, recent studies underlined that their significance may increase in the measurement of thermal conductivity of building materials because of surface roughness [62-63]. Considering two contact resistances of $0.01 \text{ m}^2 \cdot \text{K} \cdot \text{W}^{-1}$ between the device and the sample, thermal conductivity may differ by approx. 3.5 %. To sum up, uncertainties range between 1 and 15 %. It presents the same order of magnitude than repeatability errors, which may be due to sample density variability. Nevertheless, the mean repeatability remains acceptable for these properties.

	Thermal conductivity λ [W.m ⁻¹ .K ⁻¹]	Water vapor diffusion resistance factor μ [-]
Dimensions	1.4 % (6.1 %)	1.5 % (5.4 %)
Potential accuracy	1 % (1 %)	14.4 % (15.9 %)
Interface resistance	3.6 % (4.5 %)	4.4 % (7.9 %)
Repeatability	4.4 % (11.7 %)	5.2 % (16.3 %)

Table 6: Mean and maximum (in brackets) errors due to repeatability and uncertainty for measurement of thermal conductivity and water vapor diffusion resistance factor.

Regarding capillary absorption tests, numerous sources of uncertainty in A-coefficient measurements were listed and analyzed in [64-66], among which initial moisture content, temperature, deviation in the experimental procedure or data processing. Beside these sources,

two others are identified for these materials: surface heterogeneity and water erosion. The second point may cause earth and even hemp shiv loss during the experiment. Consequently, mass variations against square root of time deviates from the ideal linear behavior, making the evaluation of A_w difficult. For each sample, slope is evaluated in the most linear part at the beginning of the curve (between 10 min and 4h). Finally, mean and maximal errors due repeatability are equal to 12.5 % and 22 % respectively.

4.2 Heat transfer property

Results for thermal conductivity measured after drying at 70 °C are gathered in Table 7. Figure 5 includes the additional thermal conductivity measured on samples of batch 1 after two others conditioning (drying at 40 °C or conditioning at 23 °C and 50 %RH) as function of density.

As preliminary remark, let note that heat can be theoretically transferred by conduction, convection, radiation and even phase change during the experiment. The importance of convection can be estimated by calculating the Rayleigh-Darcy number [67]. Considering air permeability in the order of 10^{-10} m^2 [17], this number is less than unity and much less than the threshold of 40: convection may be neglected with confidence regarding conduction. The importance of radiation can be estimated by calculating the Planck number [68]. Considering mean free path of photons in the order of 0.5 mm, this number is around 30 and much higher than the threshold of 10: radiation may be neglected with confidence regarding conduction. Last, phase change is obviously not considered for dry materials and negligible for materials with low moisture content [69]. Consequently, measured thermal conductivity represents heat transfer by conduction in the porous and in the solid phase.

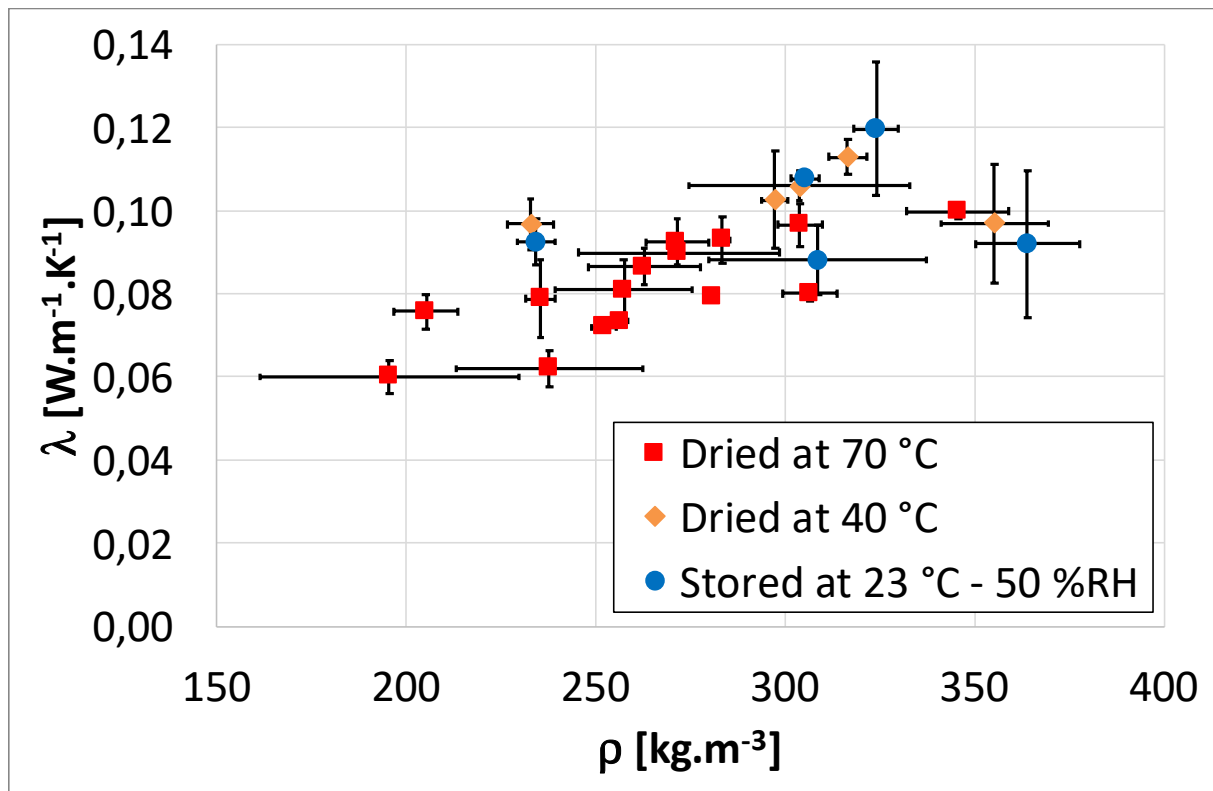


Figure 5: Thermal conductivity of light earth building materials measured after different conditioning as function of density.

As observed in Figure 5, thermal conductivity increases with density, i.e. with increasing solid fraction (resp. decreasing void fraction). Particularly, it underlines the influence formulation and of earth slip. On the other hand, no influence of hemp shiv is noted since the observed variations are lower than the confidence range. This agrees with results of Williams et al. [10], who observed also a limited effect on the internal structure. By lowering drying temperature or conditioning the samples at 23 °C and 50 %RH, moisture content, and thus density, is higher leading to higher thermal conductivity. Last, the measured values are similar to the ones presented in Table 1 and to thermal conductivity of hemp concrete [4,5,10,12,13,15,17].

4.3 Hydric transfer properties

Results for water vapor diffusion resistance factor and capillary absorption coefficient are gathered in Table 7 (except for sample E1H1a which is too crumbly for measuring capillary absorption coefficient). For both experiments, moisture can be transferred by diffusion and convection in liquid and vapor state. In dry cup experiment, no absolute pressure gradient of air or liquid water exists meaning that no transfer by convection occurs. Furthermore, relative humidity ranges at best between 5 and 50 %RH within the materials, corresponding to moisture content lower than 5 %. At this level, moisture is absorbed in the cell structure of hemp shiv or strongly adsorbed to the active surface of clays. Since no continuous liquid path is expected and due to the strong adsorption forces involved, the measured property corresponds rather to vapor diffusion through the multiscale porous structure for which open porosity and tortuosity are the main factors of influence. In the present work, material's porosity does not vary to large extent: no trend can be observed for water vapor diffusion resistance factor for which the values range between 2.24 and 4.14. These values are similar to the ones presented in Table 1 and to vapor permeability of hemp concrete [15,18,70].

In the first stage of capillary absorption test, mechanisms of moisture transfer are quite complex in which capillary forces and gravity play non-negligible role. Particularly for these materials, liquid water is expected to be transferred through the microporosity of the binder and then stored in the aggregates. Indeed, capillary absorption coefficient tends to increase as the hemp fraction decreases (or the earth fraction increases). Furthermore, hemp and earth seem to be influencing parameters. For instance, differences higher than uncertainty are observed for the three hemp (samples E0H1 to E0H3). Similarly, sample E5H1b presents the highest value: this sample has the lowest hemp fraction (see Table 4), but earth E5 has also the highest clay activity. On the other hand, the results are not clearly correlated to the density contrary to rammed earth [46]. Finally, capillary absorption coefficient range between 0.027

and

$0.135 \text{ kg}\cdot\text{m}^{-2}\cdot\text{s}^{-0.5}$ and has the same order of magnitude than the ones measured for lime-hemp concrete [15,18].

	Name	Thermal conductivity λ [W.m ⁻¹ .K ⁻¹]	Water vapor diffusion resistance factor μ [-]	Capillary absorption coefficient A_w [kg.m ⁻² .s ^{-0.5}]
Batch 1	E0H1	0.097 ± 0.005	3.14 ± 0.20	0.058 ± 0.003
	E0H2	0.093 ± 0.005	2.90 ± 0.33	0.046 ± 0.004
	E0H3	0.100 ± 0.002	3.43 ± 0.13	0.036 ± 0.008
	E0H1(L)	0.076 ± 0.004	3.04 ± 0.15	0.031 ± 0.004
	E0H1(S)	0.090 ± 0.000	2.24 ± 0.37	0.134 ± 0.03
Batch 2	E1H1a	0.060 ± 0.004	3.84 ± 0.20	-
	E1H1b	0.062 ± 0.004	3.27 ± 0.27	0.089 ± 0.013
	E2H1a	0.079 ± 0.009	3.86 ± 0.17	0.046 ± 0.005
	E2H1b	0.079 ± 0.001	3.66 ± 0.10	0.058 ± 0.007
	E3H1a	0.092 ± 0.006	4.14 ± 0.08	0.027 ± 0.003
	E3H1b	0.086 ± 0.004	3.74 ± 0.15	0.037 ± 0.005
	E4H1a	0.072 ± 0.001	3.77 ± 0.21	0.068 ± 0.008
	E4H1b	0.073 ± 0.001	3.77 ± 0.23	0.073 ± 0.008
	E5H1a	0.081 ± 0.007	3.82 ± 0.23	0.079 ± 0.017
	E5H1b	0.080 ± 0.002	4.01 ± 0.06	0.135 ± 0.011

Table 7: Transfer properties of light earth building materials.

5 Conclusions

This work focused on the hygrothermal properties of light-earth building materials made of hemp shiv and earth slip. Experiments were carried out on 3 hemp shiv, 6 earth and 15 mixtures in the view of evaluating material variability. Besides, attention is also paid on protocols and methods in the view of comparing this variability with other sources of uncertainty. Main results are sum-up in Table 8.

Parameter	Min	Max	Maximal uncertainty/variability	Main source of uncertainty
ρ_{dry} [kg.m ⁻³]	194	345	34	Material variability
Porosity [-]	0.83	0.893	0.019	Material variability
c_{p_dry} [J.kg ⁻¹ .K ⁻¹]	965	1105	120	Drying T / RH
w_{80} [kg.kg ⁻¹]	0.0531	0.0756	0.02	Drying T / RH
λ_{dry} [W.m ⁻¹ .K ⁻¹]	0.06	0.1	0.01	Measurement repeatability
μ [-]	2.24	4.14	0.4	Measurement repeatability
A_w [kg.m ⁻² .s ^{-0.5}]	0.027	0.135	0.017	Measurement repeatability

Table 8: Hygrothermal properties of light-earth building materials investigated in the present study.

Regarding thermal and hygric storage properties, results indicate that drying temperature and drying relative humidity (to a lesser extend) are the most influencing parameters, particularly on the moisture content determination. As expected, different characterization methods lead to different results since their initial conditioning protocols are not strictly identical. However, no conclusions can be drawn regarding the best method. Particularly, a deeper analysis on the effect of drying temperature on material stability is required. Last, the

material variability is evaluated to 3.5 % for specific heat capacity and to 16 % for moisture content at 80 %RH and is in the same order of magnitude than above-mentioned uncertainties. Furthermore, it was found that using a mixing law lead to satisfying results. This point is interesting in the view of speed up the characterization, since the measurement on constitutive materials takes less time.

Regarding thermal and hygric transfer properties, following results are found: thermal conductivity ranges between 0.06 and 0.12 $\text{W}\cdot\text{m}^{-1}\cdot\text{K}^{-1}$ and clearly depends on the density, but also on relative humidity and drying temperature; water vapor diffusion resistance factor ranges between 2.24 and 4.14 and capillary absorption coefficient ranges between 0.027 and 0.135 $\text{kg}\cdot\text{m}^{-2}\cdot\text{s}^{-0.5}$. Even if measurement repeatability is the main source of uncertainty, it is still lower than material variability.

Based on these results, light-earth can be used in building envelope to insure quite high insulation level and to provide thermal inertia, but also to properly moderate indoor humidity variations compared to conventional construction methods. Hygrothermal simulation could support these assessments.

6 Acknowledgement

This study is a part of the ECO-TERRA project (Development of light earth construction materials for efficient green buildings), with the support of ADEME, Fondation de France, Brittany and Normandy Regions and French Ministry of Education and Research.

7 References

- [1] Amziane, S., & Collet, F. (Eds.). (2017). Bio-aggregates based building materials: state-of-the-art report of the RILEM Technical Committee 236-BBM (Vol. 23). Springer.
- [2] Laborel-Préneron, A., Magniont, C., & Aubert, J. E. (2018). Characterization of barley straw, hemp shiv and corn cob as resources for bioaggregate based building materials. *Waste and biomass valorization*, 9(7), 1095-1112.
- [3] Labat, M., Magniont, C., Oudhof, N., & Aubert, J. E. (2016). From the experimental characterization of the hygrothermal properties of straw-clay mixtures to the numerical assessment of their buffering potential. *Building and Environment*, 97, 69-81.
- [4] Pierre, T., Colinart, T., & Glouannec, P. (2014). Measurement of thermal properties of biosourced building materials. *International Journal of Thermophysics*, 35(9-10), 1832-1852.
- [5] Gourlay, E., Glé, P., Marceau, S., Foy, C., & Moscardelli, S. (2017). Effect of water content on the acoustical and thermal properties of hemp concretes. *Construction and Building Materials*, 139, 513-523.
- [6] Berger, J., Guernouti, S., Woloszyn, M., & Buhe, C. (2015). Factors governing the development of moisture disorders for integration into building performance simulation. *Journal of Building Engineering*, 3, 1-15.
- [7] www.wufi.de
- [8] <http://bauklimatik-dresden.de/delphin/index.php>
- [9] Woloszyn, M., & Rode, C. (2008). Tools for performance simulation of heat, air and moisture conditions of whole buildings. *Building Simulation*, 1 (1), 5-24.
- [10] Williams, J., Lawrence, M., & Walker, P. (2018). The influence of constituents on the properties of the bio-aggregate composite hemp-lime. *Construction and Building Materials*, 159, 9-17.

- [11] Delannoy, G., Marceau, S., Glé, P., Gourlay, E., Guéguen-Minerbe, M., Diafi, D., Nour, I., Amziane, S., & Farcas, F. (2019). Influence of binder on the multiscale properties of hemp concretes. *European Journal of Environmental and Civil Engineering*, 23(5), 609-625.
- [12] Collet, F. (2017). Hygric and Thermal Properties of Bio-aggregate Based Building Materials. In *Bio-aggregates Based Building Materials* (pp. 125-147). Springer, Dordrecht.
- [13] Williams, J., Lawrence, M., & Walker, P. (2017). The influence of the casting process on the internal structure and physical properties of hemp-lime. *Materials and Structures*, 50(2), 108.
- [14] Palumbo, M., Lacasta, A. M., Holcroft, N., Shea, A., & Walker, P. (2016). Determination of hygrothermal parameters of experimental and commercial bio-based insulation materials. *Construction and Building Materials*, 124, 269-275.
- [15] Walker, R., & Pavía, S. (2014). Moisture transfer and thermal properties of hemp–lime concretes. *Construction and Building Materials*, 64, 270-276.
- [16] Mazhoud, B., Collet, F., Pretot, S., & Chamoin, J. (2016). Hygric and thermal properties of hemp-lime plasters. *Building and Environment*, 96, 206-216.
- [17] Seng, B., Magniont, C., & Lorente, S. (2018). Characterization of a precast hemp concrete block. Part I: Physical and thermal properties. *Journal of Building Engineering*.
- [18] Seng, B., Magniont, C., & Lorente, S. (2018). Characterization of a precast hemp concrete block. Part II: Hygric properties. *Journal of Building Engineering*.
- [19] Prétot, S., Collet, F., & Garnier, C. (2014). Life cycle assessment of a hemp concrete wall: Impact of thickness and coating. *Building and Environment*, 72, 223-231.
- [20] Laborel-Preneron, A., Aubert, J. E., Magniont, C., Tribout, C., & Bertron, A. (2016). Plant aggregates and fibers in earth construction materials: A review. *Construction and Building Materials*, 111, 719-734.

- [21] Goodhew, S., & Griffiths, R. (2005). Sustainable earth walls to meet the building regulations. *Energy and Buildings*, 37(5), 451-459.
- [22] Busbridge, R. and Rhydwen, R. (2010). An investigation of the thermal properties of hemp and clay monolithic walls. Proceedings of Advances in Computing and Technology, (AC&T) The School of Computing and Technology 5th Annual Conference, University of East London, pp.163-170.
- [23] Mazhoud, B., Collet, F., Pretot, S., & Lanos, C. (2018). Development and hygric and thermal characterization of hemp-clay composite. *European Journal of Environmental and Civil Engineering*, 22(12), 1511-1521.
- [24] Holzhueter, K., & Itonaga, K. (2017). The Potential for Light Straw Clay Construction in Japan: An Examination of the Building Method and Thermal Performance. *Journal of Asian Architecture and Building Engineering*, 16(1), 209-213.
- [25] Niang, I., Maalouf, C., Moussa, T., Bliard, C., Samin, E., Thomachot-Schneider, C., Lachi, M., Pron, H., Mai, T.H., & Gaye, S. (2018). Hygrothermal performance of various Typha–clay composite. *Journal of Building Physics*, 42(3), 316-335.
- [26] Brouard, Y., Belayachi, N., Hoxha, D., Ranganathan, N., & Méo, S. (2018). Mechanical and hygrothermal behavior of clay–Sunflower (*Helianthus annuus*) and rape straw (*Brassica napus*) plaster bio-composites for building insulation. *Construction and Building Materials*, 161, 196-207.
- [27] Hamard, E., Lemercier, B., Cazacliu, B., Razakamanantsoa, A., & Morel, J. C. (2018). A new methodology to identify and quantify material resource at a large scale for earth construction–Application to cob in Brittany. *Construction and Building Materials*, 170, 485-497.
- [28] Cagnon, H., Aubert, J. E., Coutand, M., & Magniont, C. (2014). Hygrothermal properties of earth bricks. *Energy and Buildings*, 80, 208-217.

- [29] Vincelas, T. (2019). Caractérisation d'éco-matériau Terre Chanvre en prenant en compte la variabilité des ressources disponibles localement, Phd. Thesis, Université de Bretagne Sud, Lorient.
- [30] Meunier, A. (2005). Clays. Springer Science & Business Media.
- [31] Chen, C. W., Gaudefroy, V., Duc, M., Descantes, Y., Hammoum, F., & Magnan, J. P. (2016). A mineralogical approach of the interactions between bitumen, clay and water in hot mix asphalt (HMA). In 8th RILEM International Symposium on Testing and Characterization of Sustainable and Innovative Bituminous Materials (pp. 61-72). Springer, Dordrecht.
- [32] Degrave-Lemeurs, M., Glé, P., & de Menibus, A. H. (2018). Acoustical properties of hemp concretes for buildings thermal insulation: Application to clay and lime binders. *Construction and Building Materials*, 160, 462-474.
- [33] Picandet, V. (2013). Characterization of Plant-Based Aggregates. In *Bio-aggregates Based Building Materials* (pp. 27-74). Springer, Dordrecht.
- [34] Vincelas, T., Lecompte, T., Hamard, E., de Menibus, A. H., Lenormand, H., Colinart, T. (2019). Methods to evaluate earth slip cohesion to build with light earth. Accepted for publication in *Construction and Building Materials*
- [35] ISO 12570 (2000) – Hygrothermal performance of building materials and products -- Determination of moisture content by drying at elevated temperature.
- [36] ISO 12570/A1 (2013) – Hygrothermal performance of building materials and products — Determination of moisture content by drying at elevated temperature - Amendment 1.
- [37] ISO 12570/A2 (2018) – Hygrothermal performance of building materials and products — Determination of moisture content by drying at elevated temperature - Amendment 2.
- [38] ISO 11464 (2006) – Soil quality - Pretreatment of samples for physico-chemical analysis.

- [39] EN 14063-1 (2016) – Thermal insulation products for buildings. In-situ formed expanded clay lightweight aggregate products. Specification for the loose-fill products before installation.
- [40] EN 13171 (2012) – Thermal insulation products for buildings. Factory made wood fibre (WF) products. Specification.
- [41] ISO 13061-1 (2014) – Physical and mechanical properties of wood. Test methods for small clear wood specimens. Determination of moisture content for physical and mechanical tests.
- [42] Nilsson, L. O., Nilsson, L. O., & Jacobs. (2018). *Methods of Measuring Moisture in Building Materials and Structures*. Springer International Publishing.
- [43] ISO 12571 (2013). Hygrothermal performance of building materials and products – Determination of hygroscopic sorption properties.
- [44] ISO 11357-4 (2014) – Plastics. Differential scanning calorimetry (DSC). Determination of specific heat capacity.
- [45] Carré, P., & Le Gall, R. (1990). Définition et détermination des conductivités thermiques dans les structures multicouches CVR–balsa. *Revue générale de thermique*, 340.
- [46] EN 12664 (2001) – Thermal performance of building materials and products. Determination of thermal resistance by means of guarded hot plate and heat flow meter methods. Dry and moist products of medium and low thermal resistance.
- [47] ISO 12572 (2016). Hygrothermal performance of building materials and products— Determination of water vapour transmission properties.
- [48] ISO 15148 (2003) – Hygrothermal performance of building materials and products. Determination of water absorption coefficient by partial immersion.

- [49] Fabbri, A., Soudani, L., McGregor, F., & Morel, J. C. (2019). Analysis of the water absorption test to assess the intrinsic permeability of earthen materials. *Construction and Building Materials*, *199*, 154-162.
- [50] Bui, R., Labat, M., & Aubert, J. E. (2017). Comparison of the Saturated Salt Solution and the Dynamic Vapor Sorption techniques based on the measured sorption isotherm of barley straw. *Construction and Building Materials*, *141*, 140-151.
- [51] Waples, D. W., & Waples, J. S. (2004). A review and evaluation of specific heat capacities of rocks, minerals, and subsurface fluids. Part 1: Minerals and nonporous rocks. *Natural resources research*, *13*(2), 97-122.
- [52] Skauge, A., Fuller, N., & Hepler, L. G. (1983). Specific heats of clay minerals: sodium and calcium kaolinites, sodium and calcium montmorillonites, illite, and attapulgite. *Thermochimica Acta*, *61*(1-2), 139-145.
- [53] Woodruff, W. F., & Revil, A. (2011). CEC-normalized clay-water sorption isotherm. *Water Resources Research*, *47*(11).
- [54] Arthur, E. (2017). Rapid estimation of cation exchange capacity from soil water content. *European Journal of Soil Science*, *68*(3), 365–373.
- [55] Thybring, E. E. (2014). Explaining the heat capacity of wood constituents by molecular vibrations. *Journal of materials science*, *49*(3), 1317-1327.
- [56] Kulasinski, K. (2015). *Physical and mechanical aspects of moisture adsorption in wood biopolymers investigated with atomistic simulations* (Doctoral dissertation, ETH Zurich).
- [57] Englund, E. T., Thygesen, L. G., Svensson, S., & Hill, C. A. (2013). A critical discussion of the physics of wood–water interactions. *Wood science and technology*, *47*(1), 141-161.

- [58] Jiang, Y., Lawrence, M., Hussain, A., Ansell, M., & Walker, P. (2019). Comparative moisture and heat sorption properties of fibre and shiv derived from hemp and flax. *Cellulose*, 26(2), 823-843.
- [59] Pazera, M., & Salonvaara, M. (2009). Examination of stability of boundary conditions in water vapor transmission tests. *Journal of Building Physics*, 33(1), 45-64.
- [60] Mukhopadhyaya, P., Kumaran, K., Lackey, J., & van Reenen, D. (2007). Water vapor transmission measurement and significance of corrections. In *Heat-Air-Moisture Transport: Measurements on Building Materials*. ASTM International.
- [61] Vololonirina, O., & Perrin, B. (2016). Inquiries into the measurement of vapour permeability of permeable materials. *Construction and Building Materials*, 102, 338-348.
- [62] Clarke, R. E., Shabani, B., & Rosengarten, G. (2017). Interface resistance in thermal insulation materials with rough surfaces. *Energy and Buildings*, 144, 346-357.
- [63] Yoon, S., Macphee, D. E., & Imbabi, M. S. (2014). Estimation of the thermal properties of hardened cement paste on the basis of guarded heat flow meter measurements. *Thermochimica acta*, 588, 1-10.
- [64] Bomberg, M., Pazera, M., & Plagge, R. (2005). Analysis of selected water absorption coefficient measurements. *Journal of Thermal Envelope and Building Science*, 28(3), 227-243.
- [65] Feng, C., Janssen, H., Feng, Y., & Meng, Q. (2015). Hygric properties of porous building materials: Analysis of measurement repeatability and reproducibility. *Building and Environment*, 85, 160-172.
- [66] Feng, C., & Janssen, H. (2018). Hygric properties of porous building materials (III): Impact factors and data processing methods of the capillary absorption test. *Building and Environment*, 134, 21-34.

- [67] Nield, D. A., & Bejan, A. (2006). *Convection in porous media*(Vol. 3). New York: springer.
- [68] Ozisik, M. N. (1973). Radiative transfer and interactions with conduction and convection(Book- Radiative transfer and interactions with conduction and convection.). *New York, Wiley-Interscience, 1973. 587 p.*
- [69] Colinart, T., Pierre, T., & Glouannec, P. (2013). Prise en compte des transferts de masse dans la détermination de la conductivité thermique de matériaux bio-sourcés. In *Congrès Société Française de Thermique* (p. 1).
- [70] Lelievre, D., Colinart, T., & Glouannec, P. (2014). Hygrothermal behavior of bio-based building materials including hysteresis effects: Experimental and numerical analyses. *Energy and Buildings*, 84, 617-627.

8 Annex 1

Figure 6 and Figure 7 present respectively sorption isotherms of reference earth E0 and hemp shiv H1 for different drying protocol and different measurement techniques. Particularly, Figure 7 includes results obtained on a second DVS equipment (SPS-x). This device can monitor simultaneously up to 23 samples of approximately 1 g. Here, the experimental protocol is the following: sample is first dried at 105 °C; then, the relative humidity was increased in steps of 10% from 0 to 90% and decreased on 0 again, the temperature being set to 23 °C. As the limit for the change to another humidity level a maximal mass variation of 0.01% in 15 min was defined.

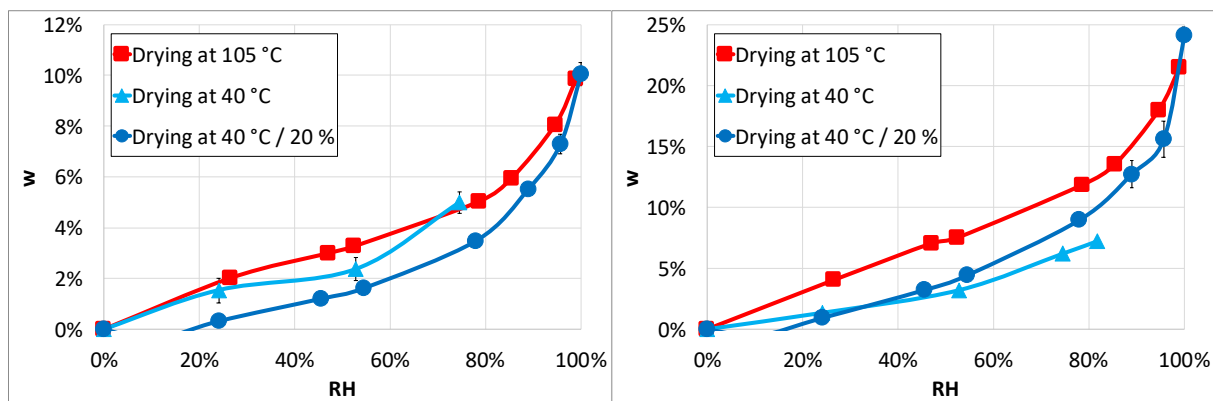


Figure 6: Sorption isotherms of reference earth E0 (a) and hemp shiv H1 (b) for different drying protocols.

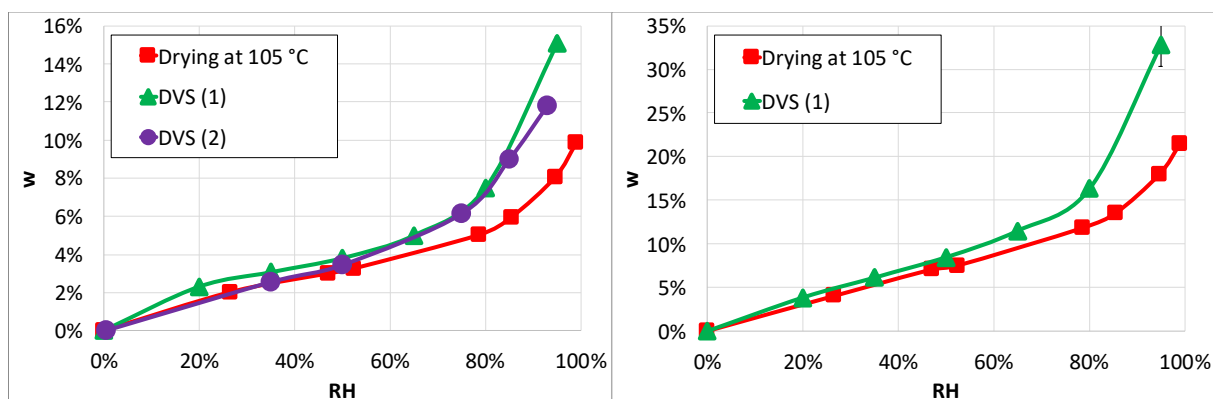


Figure 7: Sorption isotherms of reference earth E0 (a) and hemp shiv H1 (b) for different measurement technique.

Figure 8 present the measured and the estimated (from the mixing law) sorption isotherms for samples E0H1 and E1H1.

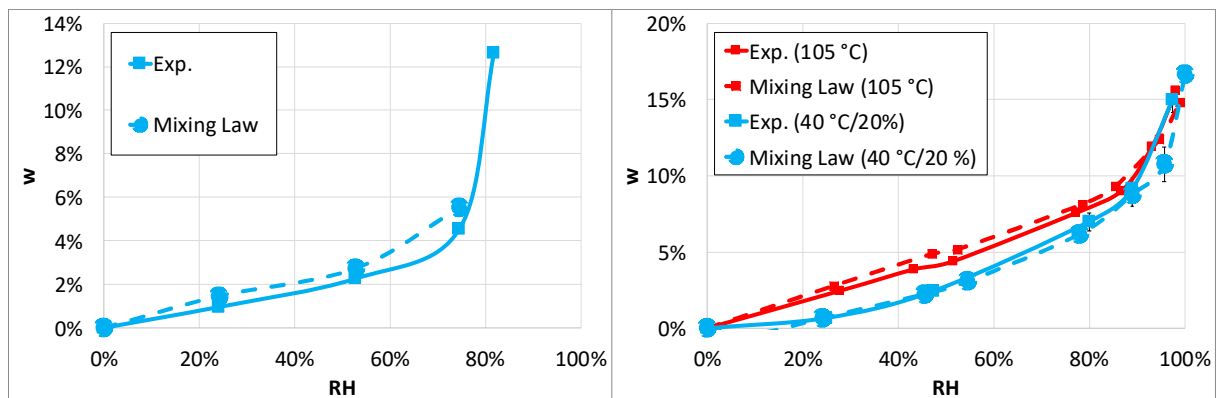


Figure 8: Sorption isotherms of samples E0H1 and E1H1a.